Differential scanning calorimetry-based investigations of erythritol – sodium chloride phase change composites for thermal energy storage

Paul Gregory Felix, Velavan Rajagopal and Kannan Kumaresan

PSG College of Technology, Coimbatore, India

Abstract

Low thermal conductivity of organic phase change materials (PCMs) for thermal energy storage systems induces the necessity to apply suitable heat transfer enhancement techniques for these materials. The purpose of this study was to improve thermal conductivity of a PCM erythritol by using sodium chloride as an additive, such that the material can be applied for steam cooking systems when integrated with solar parabolic trough collectors. In this study, erythritol-NaCl composites were synthesized by using the melting method, and the key physicochemical properties of the composites were estimated by using differential scanning calorimetry (DSC) coupled with thermo-gravimetric analysis (TGA). The observations indicate that there has been a significant improvement in the thermal conductivity of erythritol supplemented with NaCl. Further, thermal behaviour of the material indicates that it is suitable for steam cooking applications. Furthermore, mathematical models based on the experimental observations can be potentially utilized for further studies of erythritol-NaCl composites.

Keywords: composites; latent heat storage; mathematical modelling; steam cooking; thermal conductivity.

Available on-line at the Journal web address: http://www.ache.org.rs/HI/

ORIGINAL SCIENTIFIC PAPER

UDC: 616-073.66:(547.427.1+ 661.833`032.1)

Hem. Ind. **76 (1)** 5-18 (2022)

1. INTRODUCTION

Parabolic trough collectors (PTCs) find applications in cooking using solar energy and have potential benefits in elimination of green house gases (GHGs) [1-4]. Thermal energy storage (TES) systems when integrated with such PTCs [5-8] can be a potential technology for steam cooking over 24 h. Phase change materials (PCMs) can serve as potential TES media for this application owing to their latent heat storage [9]. PCMs store and release energy by virtue of their latent heat of phase transition without any significant temperature change, so that PCMs can store higher heat amounts than the sensible TES systems [10]. To be specific, organic PCMs exhibit stable melting and solidification cycles [11] at a broad spectrum of phase transition temperatures [12], possess significant latent heat of phase transition [13], are non-toxic [14], do not exhibit supercooling [13-15] and resistant to corrosion [16]. It has been identified that such organic PCMs when integrated with steam cooking systems can convert the complete steam cooking process to rely on renewable energy sources and, further, the higher latent heat of fusion of such materials will reduce the system size, since the higher latent heat of phase transition, the lower will be the quantity of PCM required. Among the various organic PCMs, erythritol ((2*R*,3*S*)-butane-1,2,3,4-tetrol [17]), as a PCM, gains importance. Erythritol ($C_4H_{10}O_4$) is a sugar alcohol [18] that can be suitable for medium temperature applications [19] as well as for solar TES applications owing to its high volume latent heat of 502.9 J cm^{-3} [20]. Next, from a steam cooking perspective, a PCM will be suitable for steam generation only if its melting temperature lies between 110-130 °C, so that the output steam can be maintained at a minimum of 100 °C. When erythritol is considered, it has a satisfactory latent heat of fusion values [21] and a melting point [22] suitable for the application. Furthermore, since erythritol is a food additive [23], it is conveniently safe to use in operation for steam cooking.

Still, it has been noted that a drawback of organic PCMs is in lower thermal conductivities, which can result in higher thermal resistances [24-26]. High thermal resistances would hinder the heat transfer through the material, resulting in

Corresponding authors: Paul Gregory Felix, PSG College of Technology, Coimbatore, India; Tel. +91-9629431403
E-mail: 1807rm01@psgtech.ac.in
Paper received: 26 May 2021; Paper accepted: 11 February 2022; Paper published: 25 February 2022.
https://doi.org/10.2298/HEMIND210526003F

longer charging times. Charging time is the time required for the material to heat from its ambient temperature to the desired temperature (post-melting). Erythritol, being an organic PCM, does not present an exception exhibiting low thermal conductivity [27,28]. For example, in an experimental study on erythritol as a PCM filling annular space of a shell-and-tube unit (between the cylinders of 45 mm OD and 100 mm ID and height of 900 mm), it was observed that approximately 12 h was needed for erythritol to completely charge [29]. Hence thermal conductivity improvement is required as the PCM should be charged within daytime, as the charging process is dependent on solar PTCs. In this direction, addition of high thermal conductivity additives to the base PCM has been reported as one of the promising methods [30]. In such a way phase change composites (PCCs) are obtained. For improvement the erythritol thermal conductivity different additives were investigated such as expanded graphite [27], percolated aluminium filler [31], modified carbon nanotubes [28], vermiculate with graphite [32], spherical graphite [33], and nickel nanoparticles [33]. Researchers have also synthesized PCCs based on erythritol by addition of copper, aluminium, SiO_2, and TiO_2 nanoparticles individually, which led to significant improvements in the thermal conductivity [34]. However, all of the aforementioned additives require at least to some extent specialized chemical preparation and processing techniques, and hence a readily available additive will be less complex in the PCC synthesis as well as more economical.

Preliminary literature search shows that physicochemical properties of sodium chloride (NaCl) are convincingly appropriate to be used as an additive to erythritol, which has hardly been investigated so far. The key physicochemical properties of NaCl are presented in Table 1.

Table 1. Physico-chemical properties of NaCl

Property	Magnitude	Reference
Specific heat, kJ kg^{-1} K^{-1}	0.88	[35]
Density, kg m^{-3}	2176	[36]
Thermal conductivity, W m^{-1} K^{-1}	6.1 at 30 °C; 3.5 at 140 °C	[37]
Melting temperature, °C	803.4	[38]

Hence, this study commenced with a hypothesis that, addition of NaCl as a higher thermal conductivity material than erythritol, will improve the overall thermal conductivity of the resulting PCC. Furthermore, NaCl being non-toxic can be conveniently used for steam cooking applications as it will not be harmful if any leaks or accidents occur in the system. Therefore, in this study, erythritol-NaCl PCCs were synthesized and experimentally investigated regarding intended thermal conductivity improvements. Also, parametric mathematical models were built using the estimated parameters to aid researchers to perform numerical studies on erythritol-NaCl PCCs.

2. MATERIALS AND METHODS

2. 1. Study design

This study was conducted in three phases comprising: the synthesis of the erythritol-based PCCs, estimation of key physicochemical properties of the synthesized PCCs, and, ultimately, mathematical modelling to map variations in the key physicochemical properties as shown in Figure 1. Firstly, a certain quantity of pure erythritol was subjected to controlled heating (until complete melting) by using an electric heater followed by cooling such that the melting and solidification behavior could be observed. Further, as it was previously reported [39] that pure erythritol undergoes a mass loss when heated beyond approximately 220 °C, we have also verified such behavior of the material. Following preliminary investigations, erythritol-based PCCs were then synthesized, and the key physicochemical properties were estimated experimentally by using differential scanning calorimetry (DSC) and thermo-gravimetric analysis (TGA). The obtained results were used to derive mathematical models for deeper interpretation.

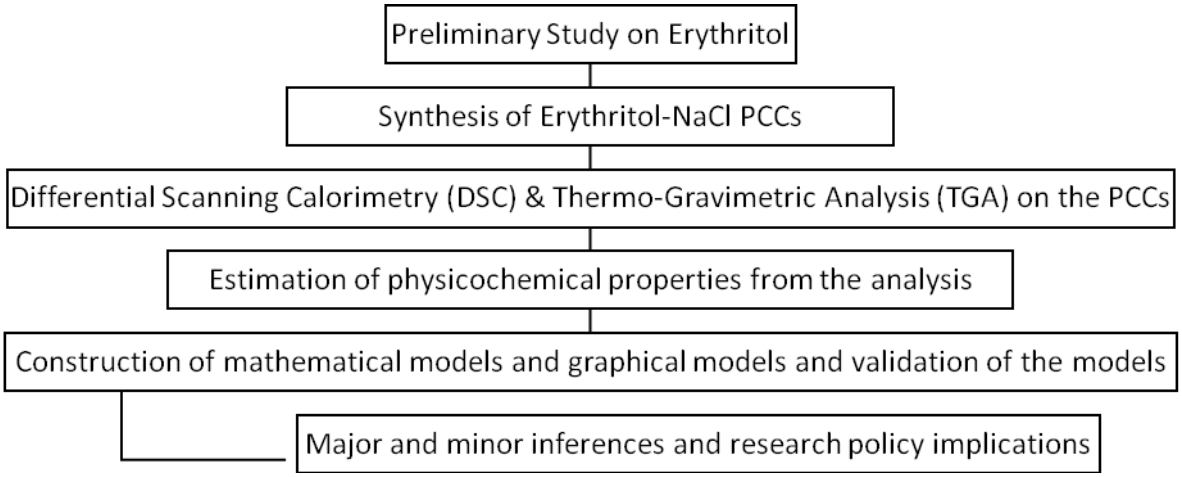

Figure 1. A schematic representation of the study design adopted in the present work

2. 2. Synthesis of the PCCs

Erythritol-NaCl PCCs were synthesized at four different NaCl mass contents: 10, 20, 30 and 40 %. The composition was designed so that the obtained composite would exhibit both the latent heat of fusion of pure erythritol as well as the high thermal conductivity of NaCl. Analytical grade erythritol with 99 % purity was procured from Shandong Sanyuan Biotechnology, China for the synthesis and used without any further chemical and physical processing. Also, industry-grade NaCl (Baba Chemicals, India) was utilized for the synthesis as commercial and edible grade NaCl are not recommended due to possible iodized form. All PCCs were synthesized by adopting the melting method from literature [40,41] so that NaCl was added to erythritol in molten state. A detailed schematic presentation of the procedure that was adopted for the synthesis of all PCCs is presented in Figure 2.

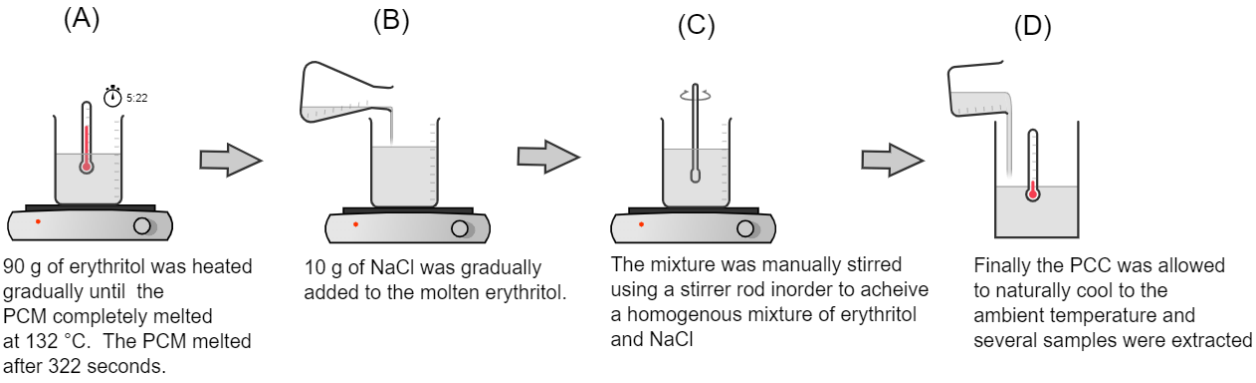

Figure 2. This illustration depicts the synthesis methodology adopted in this current study. In this procedure a 1000 W hot-plate apparatus (Sigma, India) was utilized for heating. All of the synthesis procedures were carried out at PSG College of Technology and for each PCC synthesized, five sets of replicate experimentations were carried out.

2. 3 Estimation of physicochemical properties of the obtained PCCs

All of the synthesized PCCs were subjected to DSC-TGA experimental analysis. During the DSC-TGA procedure, the sample PCC was placed in an aluminium crucible and both materials were subjected to uniform heating, temperature development was monitored, and the resulting heat flux magnitudes were recorded. All DSC-TGA experimental analyses were performed by using a NETZSCH STA 449F3 STA449F3A-1100-M apparatus (NETZCH, Germany). Uniform heating rate of 10 K min^{-1} was applied in all investigations and all experiments were carried out in an N_2 environment. All samples were subjected to the analysis up to 300 °C. High-temperature studies were not necessary in the present case since the synthesized PCCs are intended for TES applications for steam cooking purposes, and thus will not be subjected to very high temperatures. DSC-TGA analyses served to plot the heat flux (ϕ) and the sample mass in respect to the initial mass

(m_{pcc}) as functions of the PCC temperature (T). A sample curve for the heat flux profile recorded for the erythritol sample is presented in Figure 3 for illustration.

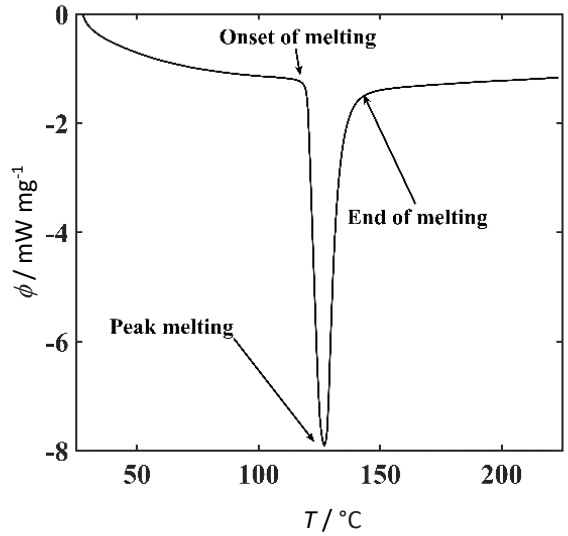

Figure 3. An illustration of the DSC heat flux profile (obtained for erythritol sample) for interpretation

From the heat flux profile, the peaking zone was identified as the phase transition zone [42] and the corresponding melting temperatures were recorded. Further, the area under the melting curve (A_m) was utilized to estimate the latent heat of fusion (λ) of the sample. The mathematical formulation utilized to estimate the latent heat magnitude from the DSC observation is presented by the equation (1):

$$\lambda = \frac{A_m}{\frac{\delta T}{\delta t}} \tag{1}$$

The activation energy (E_a) was estimated by adopting the Coats-Redfurn method by utilizing the TGA thermogram [43]. This method has been adapted from the Arrhenius equation [44-46]. In this method, the first order reaction is represented as in equation (2):

$$\log\left(\frac{-\log(1-\alpha)}{T^2}\right) = \log\frac{AR_m}{\beta' E_a}\left(1-\frac{2RT}{E_a}\right) - \frac{E_a}{2.303RT} \tag{2}$$

In the equation, α denotes the instantaneous fraction of the sample decomposed, A denotes the frequency factor, R is the universal gas constant and β' is the employed heating rate (in the TGA process). In the Eq. (2), the term E_a / 2.3030R was estimated by estimating the slope of the plot of log [-log (1-α)/T^2] *vs.* 1000/T. Then, the activation energy (E_a) was estimated by applying the equation (3):

$-E_a/2.303R$ = Slope (3)

Thermal conductivities for all compositions were estimated by adopting the thermal resistance methodology. This method is based on the fundamental thermal conductivity equation as shown in the equation (4):

$Q = k\,(\delta T/L)\,A_{CS}$ (4)

This methodology has previously been adopted by several researchers to estimate the thermal conductivity magnitudes from the DSC-TGA thermograms [47-49]. In this approach a plot of the differential power in DSC-TGA (ΔP) and the programmed temperature (T_{pr}) was determined, and the slope was equated to the thermal resistance (R_c) by adopting the equation (5):

$$\frac{d\Delta P}{dT_p} = \frac{2}{R_c} \tag{5}$$

Further, the thermal conductivity was estimated for each composition by utilising the equation (6):

$$R_c = \frac{l^h}{k_{s/l} A_{CS}} \tag{6}$$

The procedure was performed individually for solid temperature and liquid temperature ranges and ultimately the solid phase and liquid phase thermal conductivities were obtained. In the equations, k represents the thermal conductivity, A_{cs} represents the cross-sectional area of the material, l^h represents the height of the sample when placed in the DSC-TGA apparatus. Dimensions of the aluminium crucible equipped was utilised to estimate the dimensional parameters required to estimate the thermal resistance R_c.

Further, the liquid fraction (β) was estimated by utilizing the model proposed by Beata *et al.* [50], as presented by the equation:

$$\beta = \begin{cases} \dfrac{T - T_{ms}}{T_{me} - T_{ms}} & T_{ms} < T < T_{me} \\ 0 & T < T_{ms} \\ 1 & T_{me} < T \end{cases} \tag{7}$$

were T_{ms} denotes the onset temperature of melting, T_{me} denotes the completion temperature of melting. Also, the apparent heat capacity (C) was estimated independent of the mass by correlating the heat flux (ϕ), temperature (T), and time (t), by using the equation (8):

$$C = \phi\, t \,/\, T \tag{8}$$

For the above correlation, the instantaneous heat flux magnitudes recorded by the DSC-TGA apparatus were utilised together with the corresponding instantaneous temperature. Further, the time needed for the sample to reach that particular temperature was also recorded and was utilised in the estimation.

The charging time (t_c) expressed per unit mass of the composites was observed in order to estimate the improvement of the material functionality by addition of NaCl. In this study, the charging time was discretized into three parts for the analysis. The time taken by the PCM/PCC to rise from the ambient temperature to the onset of melting (solidus temperature) was termed as solid sensible charging time (t_{ss}) and the time taken by the material to change phase completely was termed as melting time (t_m). In other words, melting time can be considered as the time taken by the material to change from the onset melting temperature (T_{ms}) to the end melting temperature (liquidus temperature). Further, the time taken by the material to rise from the end melting temperature (T_{me}) to the desired temperature is termed as liquid sensible charging time (t_{ls}). The total charging time was estimated by the summation of the afore mentioned charging times. Since this study is intended for a TES application in a steam cooking system, in the charging time estimation the final temperature was considered to be 140 °C. It is desired for PTCs for steam cooking applications to provide steam at a temperature in the range 140-160 °C to charge the PCCs, and hence the temperature was chosen.

2. 4. Mathematical modelling of the estimated parameters

Mathematical modelling of the estimated parameters for the PCMs and PCCs was performed in order to get an insight into the material behaviour at a holistic level. The Stefan's condition for PCM mathematical modelling provides scope for individual parametric modelling of latent heat of fusion (λ), solid-phase thermal conductivity (k_s) and liquid phase thermal conductivity (k_l). The Stefan's condition is presented by the equation (9) [24]:

$$\lambda\rho\left(\frac{\mathrm{d}S(t)}{\mathrm{d}t}\right) = k_s\left(\frac{\delta T_s}{\delta t}\right) - \left(\frac{\delta T_l}{\delta t}\right) \tag{9}$$

In the present study, parametric mathematical modelling of λ, k_s and k_l was performed by using the Gauss-Newton iterative algorithm and asymptomatic regression models were applied for modelling. The general form for asymptomatic regression models (concave and convex) is presented as:

$$f(x) = \theta_1 - \theta_2\, e^{-\theta_3 m} \tag{10}$$

where θ_1, θ_2 and θ_3 represent asymptotic regression constants and m represents the content of NaCl in the composition.

3. RESULTS AND DISCUSSION

3. 1. Preliminary investigations of erythritol

Erythritol, when subjected to controlled heating was observed to thermally behave similarly to smart materials. When erythritol was heated, physical changes were absent up to 120 °C during which time the heat transfer was carried out completely by conduction. Beyond this temperature, there was a slight phase change near the bottom of the beaker, followed by considerable development in the melting front thereon. Further, during the phase change, motion of the solid and the liquid phases was observed due to the density difference, which indicates the convective heat transfer during the melting process. Change of color was not observed during the study. Upon completion of melting, erythritol appeared to be a viscous, clearly transparent liquid. Next, the liquid was allowed to naturally cool and after solidification, clear crystallite formation was observed. During solidification, the layer of the fluid facing the mouth of the beaker (in contact with air) and that in contact with the glass beaker were the first to solidify after which the solidification pattern spread out to the other parts of the material. Even though this preliminary investigation has provided an insight into the behaviour of the material; this investigation could not provide an accurate measurement of the melting temperature as the study was performed by using a conventional thermometer. The photographs of the melting and crystallization phenomena have been provided in the Supplementary material (Fig. S-1). But despite the shortcomings, heat absorption and heat releasing phenomena of the material have been well observed and this has paved the way for further intricate analysis.

3. 2. Variation in the physicochemical parameters of the PCCs

By the TGA analysis, mass losses of erythritol and all synthesized PCCs upon heating were determined. The plot of the sample mass in respect to the initial mass (m_{pcc}) *vs*. temperature is presented in Figure 4(a). It can be observed that all investigated materials behave similarly. Initiation of the significant the mass loss was only near 220 °C. If the TGA plot is intricately observed, it can be noticed that erythritol shows lower mass stability than its derivative PCCs. At 300 °C, it can be observed that there is only 20% of the residual mass of erythritol, whereas nearly 60 % residual mass for the 40 % NaCl material. For the materials with 10 and 20 % NaCl, the mass residual was 40 % , while for the 30 % NaCl material, it was nearly 25 %. The PCC with 20 % NaCl showed a profile with a sharp, though statistically insignificant drop (2.7 %) in the mass during the initial stages of heating.

The thermal degradation temperature (T_d) of the PCCs is presented in Figure 4(b) while the heat flux in Figure 4(c). A steady decrease in the heat flux during the initial stages of heating can be observed for all materials, followed by a steep descent and minimum and then another steady region. The largest minimum heat flux value was determined for erythritol while the lowest for the PCC with 40 % NaCl. In all cases, the melting zone lies between 110 and 140 °C. The area of the peak flux was evaluated and the latent heats of fusion were estimated according to the Eq. (1). The differential $(\delta T/\delta t)$ was experimentally recorded. The results are presented in Figure 4(d) showing that the latent heat of fusion decreases with the increase in the NaCl content in the PCC. From the heat flux graph, the onset of melting temperature (T_{ms}), peak melting temperature (T_{mp}), and the end melting temperature (T_{me}) were estimated (Fig. 4(e)). It can be observed that the addition of NaCl has not imposed any significant change in the melting range. Nevertheless, the fact that the magnitudes of T_{ms} for compositions of 20-40 % NaCl are lower than those for 0 and 10 % NaCl, the decrease has been considered insignificant as the difference between the highest and the lowest T_{ms} magnitude is only 5.2 %. The highest T_{ms} magnitude has been reported for 10 % NaCl (120.3 °C) case and the lowest magnitude has been reported for 40 % NaCl case (114 °C).

Activation energies were estimated by adopting Eqs. (2)-(3). The estimated activation energies are presented in the Supplementary material (Fig. S-2). All investigated PCCs have shown statistically equivalent activation energies. It should be noted that the PCCs with 20 and 30 % NaCl have shown similar magnitudes of both the latent heat of fusion and the activation energy. Solid and liquid phase thermal conductivities were calculated by using the Eq. (6). Estimated solid and liquid thermal conductivities are presented in Figure 5(a) showing significant increases in magnitudes up to nearly 3 and 2.5 times, respectively.

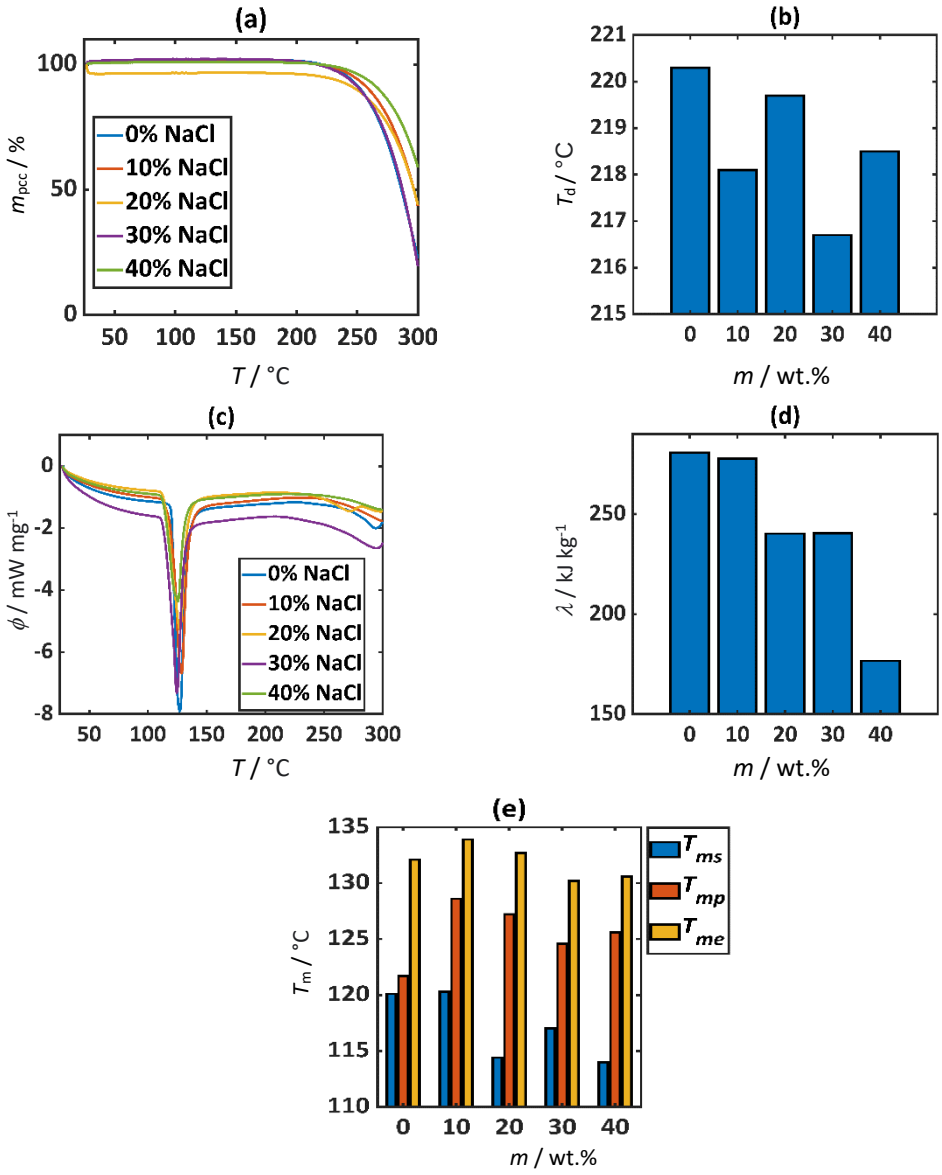

Figure 4. a - variation in the sample mass in respect to the initial mass (m_{pcc}) vs. T during the TGA analysis; b - variation in the thermal degradation temperature (T_d) with respect to the mass content of NaCl; c - variation of the instantaneous heat flux (ϕ) with temperature; d - the variation in the latent heat of fusion (λ) with respect to the mass content of NaCl; e - variation in the various melting temperatures (T_{ms}, T_{mp} and T_{me}) with respect to the mass content of NaCl. Data presents average values of 3 experimental repetitions. In the figures, m indicates the content of NaCl in erythritol

Liquid fraction profiles calculated based on experimentally determined temperature values and Eq. (7) are presented in Figure 5(b). Apparent heat capacity profiles calculated by using Eq. (8) and experimental values are presented in Figure 5(c). The heat capacities showed a sharp increase during the onset of melting and a sharp decrease during the end of melting. The T-history was generated by utilizing the equipment logger. As a uniform heating rate was provided to the material, the corresponding material temperature was also recorded. Temperature history (T-history) of the investigated materials is determined and presented in Figure 5(d). It can be observed that the PCCs exhibited faster melting than erythritol. To intricately analyse the T-history phenomenon, a specific temperature zone between 100 to 130 °C is enlarged (Fig. 5(e)) showing that the increase in NaCl content enhances the temperature increase rate of the PCCs. The T-history profile presents the duration of temperature development for one milligram of the sample. Hence it can be stated that the addition of NaCl to erythritol reduces the charging time of the obtained PCCs.

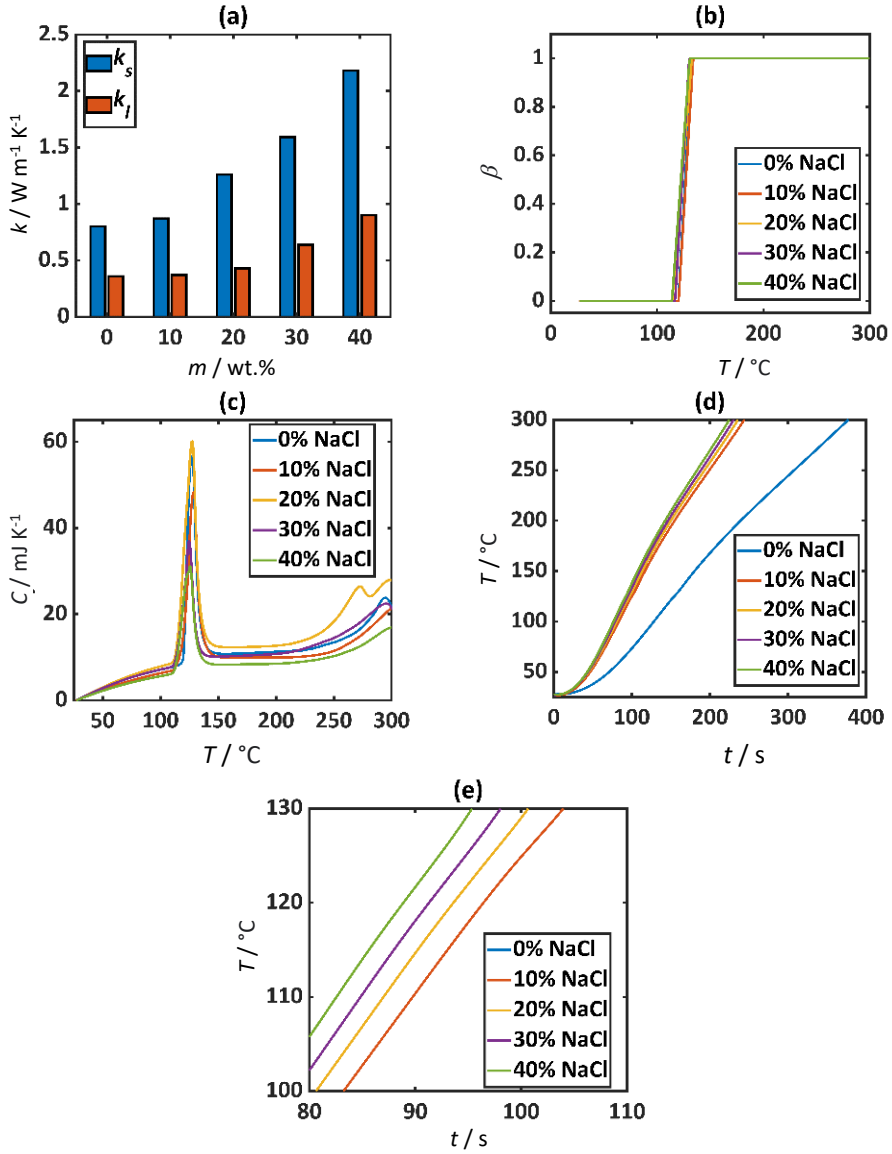

Figure 5. a - variation of solid thermal conductivity k_s and liquid thermal conductivity k_l with respect to the quantity of NaCl in erythritol; b - variation in liquid fraction (β) contour with respect to temperature; c - variation of apparent heat capacity (C) with temperature; d,e - T-history of the PCC samples. In the figures, m indicates the content of NaCl in erythritol

The total charging time per unit mass of the PCC along with times of separate charging phases is presented in Figure 6.

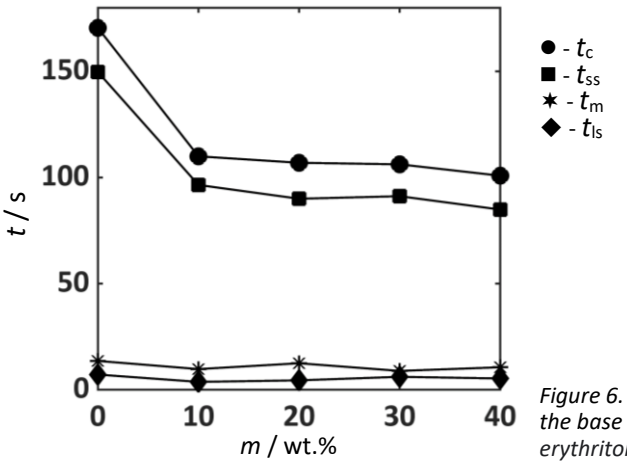

Figure 6. Variation of charging time with respect to the quantity of NaCl in the base PCM erythritol. In the figure, m indicates the content of NaCl in erythritol

From the figure, it is apparent that the charging time decreases with an increase in the NaCl fraction, and it is interesting to further note that the solid sensible time contributes the most to the overall charging time. In the Figure 6, t_{ss} denotes the solid sensible time, t_{ls} denotes the liquid sensible time, t_m denotes the melting time and t_c denotes the charging time. All time components indicate the time for one milligram of the samples. A detailed description on the various time components is provided in the Materials and Methods section

3. 3. Discussion on the thermal behaviour of the PCCs

The obtained experimental results have been compared to the observed charging times. It can be inferred that the solid thermal conductivity plays a major role in the sensible heat transfer in the PCCs. By comparing Figures 5(a) and 6, it can be noted that there is a decrease in the solid sensible charging time with a proportional increase in the solid thermal conductivity magnitude. Also, it can be observed that although there is a significant increase in the liquid thermal conductivity magnitudes, the liquid sensible time has not shown any significant change. This phenomenon is due to the basic phase change mechanism that liquid heat transfer is convection-dominated. However, the DSC-TGA analysis cannot give information on the convection magnitude. This study was commenced with a hypothesis that the addition of a higher thermal conductivity material will decrease the charging time of the resulting PCCs and the hypothesis has been validated by using the experimental observations. Table 2 presents the variation in the key physicochemical parameters of the PCCs in a more comprehensive way.

Table 2. Variations in parameters (in comparison to those of pure erythritol)

m_{NaCl} / wt.%	Increase of k_s, %	Increase of k_l, %	Decrease of λ, %	Decrease of t_c, %
10	9	6	1	36
20	58	23	14	37
30	100	82	14	37
40	173	156	37	41

The current experimental observations indicate a decrease in the latent heat with the increase in the thermal conductivity, which conforms to several literature reports. For instance, a study on nanoparticle dispersed in a PCM has shown the latent heat variation for the PCCs before and after addition of nanoparticles [51]. Also, it has been observed that the latent heat of phase transition decreases with the addition of a high thermal conductivity material in many systems studied in literature such as: eicosane - silver nanoparticle PCC, octadecane-CuO nanoparticles PCC, 1-do-decanol-graphite nanoparticles PCC, RT22-graphene nanoparticle PCC, *etc.* Similarly, in another research it was reported that addition of graphene nanoparticles to pure erythritol, there was a decrease in the latent heat with the increase in the thermal conductivity [41].

The observed heat flux profiles can be utilized as an indication of the trend of the latent heat of fusion. It can be observed from Figure 5(c), that the highest heat flux peak was achieved for erythritol (having the highest latent heat) while the lowest peak was observed for the PCC with 40 % NaCl (having the lowest latent heat). Hence, the heat flux curve can be presented as a comparative model to infer whether there is a decreasing or an increasing trend in the latent heat. However, computations have to be made to estimate the exact magnitude of the latent heat of fusion. Also, it was observed that the thermal degradation temperature (t_d) for all the composites is nearly 220 °C. From the TES application perspective, the maximal application temperature will be 140 °C and hence all the investigated PCCs are suitable for this use. Further, the estimated activation energy for all of the cases conforms to the limits of activation energy for sugar alcohols [52]. It has been observed that the magnitudes of the key physicochemical parameters estimated for erythritol conform to several literature sources, as shown in Table 3.

Table 3. Comparison of parameters for erythritol determined experimentally in the present study with literature reports.

Parameter	Current Study	Literature reports	Reference
k_s / W m^{-1} K^{-1}	0.798	0.733	[53]
k_l / W m^{-1} K^{-1}	0.357	0.326	[53]
λ / k J kg^{-1}	280.7	284 - 370	[54]
T_{mp} / °C	121.7	120.39, 120	[29],[41]

3. 4. Mathematical modelling of the parameters and discussion

To aid the solution for a typical Stefan problem, mathematical models were formulated for predictions of latent heat of fusion, solid thermal conductivity and liquid thermal conductivity. The mathematical models are presented by Eqs. (10) - (13) and the graphical form of the models is presented in Figure 7. In the equations, m represents wt.% of NaCl in the material.

$$\lambda = 289.798 - 10.0862\ e^{0.0598649m} \quad (11)$$

$$k_s = 0.387994 + 0.375957\ e^{0.03905574m} \quad (12)$$

$$k_l = 0.294262 + 0.0435885\ e^{0.0659759m} \quad (13)$$

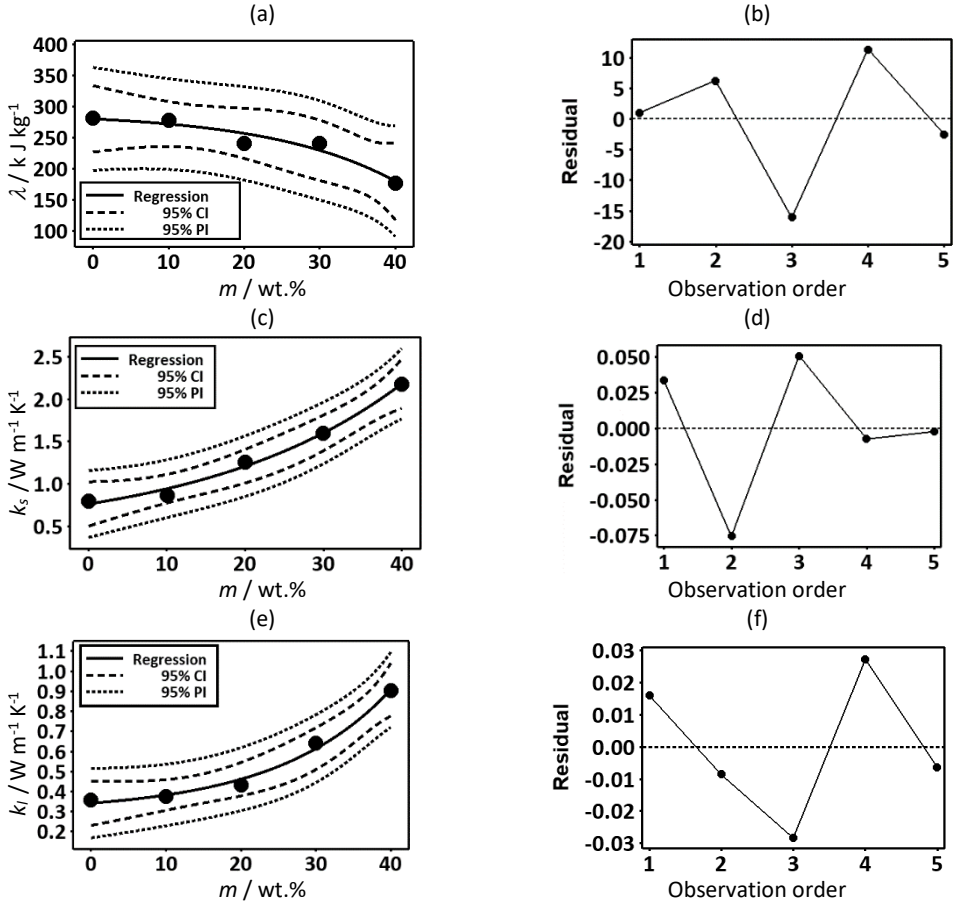

Figure 7. a - graphical form of the latent heat of fusion model; b - residuals for the latent heat of fusion model; c - graphical form of the solid thermal conductivity model. ; d - residuals for the solid thermal conductivity model; e - graphical form of the liquid thermal conductivity model; f - residuals for the liquid thermal conductivity model. In the figures, residuals indicate the difference between the observed value and the fitted value. Further, observation order indicates the index of the input wt.% magnitude of NaCl. Since there are 5 compositions, five observation orders were reported. Furthermore, CI represents the Confidence Interval and PI represents the Prediction Interval for the regressions. m indicates the content of NaCl in erythritol

As it is shown, all of the model predictions are within a 95 % confidence level and can be used as a tool to predict the behaviour of key physicochemical properties of the PCCs. From an applicability perspective, the models can be utilized for an effective system design. While selecting a specific composition of the PCC for the desired application, these mathematical models can be utilized to estimate the mass of the PCM/PCC required and thereby aid the system sizing. To facilitate optimization and to completely study the holistic behavior of the PCCs, four graphical contour models were built using the DSC-TGA observations and the constructed mathematical models (Fig. 8). The models were constructed by utilizing the distance method of interpolation and by utilizing a regular mesh for estimation [55]. Since a regular mesh and a uniform interpolation method was adopted, 5 observatory data values were sufficient for the construction of the models. The contour models plot solid thermal conductivity and liquid thermal conductivity in two

dimensions and consider the latent heat of fusion, melting time, the quantity of NaCl and peak melting temperature in the third dimension individually.

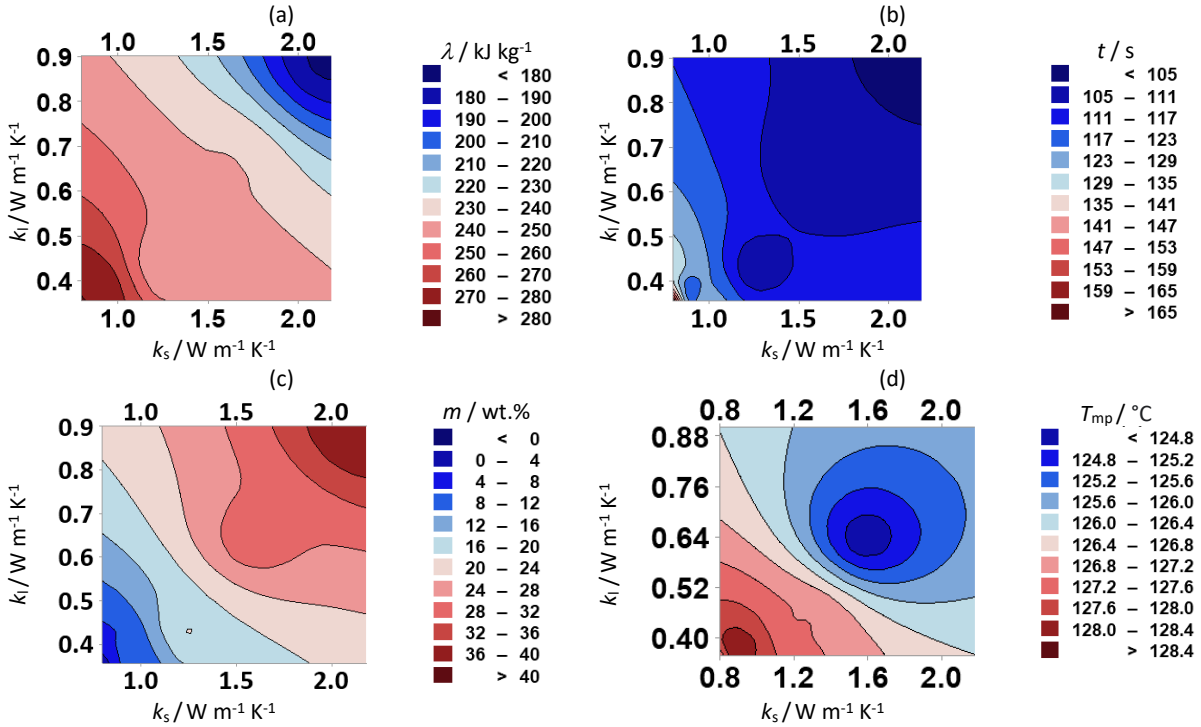

Figure 8. Contour plots of the solid (k_s) and liquid (k_l) thermal conductivities with respect to different parameters: a - latent heat of fusion (λ); b - melting time (t); c - mass content of NaCl; and d - peak melting temperature (T_{mp}). In the figures, m indicates the content of NaCl in erythritol.

From Figure 8(a), it can be inferred that lower solid thermal conductivity and lower liquid thermal conductivity are connected with a higher latent heat of fusion. Also, Figure 8(b) presents the apparent notion that the higher the thermal conductivities, the lower will be the charging time. When correlated with the contour from Figure 8(c), it can be inferred that the higher quantities of NaCl result in higher magnitudes of thermal conductivity. Figure 8(d) gains attention as it presents a unique understanding of the peak melting temperature of the NaCl containing PCCs. Since the peak melting temperature (T_{mp}) was estimated in relation to the solid and thermal conductivities, this visualisation presents an understanding from a thermal conductivity perspective. If it is compared with Figure 8(c), it can be noted that this behaviour of T_{mp} is inverse to that of the NaCl mass content behaviour. From a broader perspective, it was discussed earlier that the melting temperature was not significantly changed with the addition of NaCl. Despite insignificant magnitude changes, this contoured model has provided an insight that the higher the thermal conductivities, the lower will be the peak melting temperatures. The built contour plots are valid and reliable as they reflect the DSC-TGA observations.

4. CONCLUSION

In summary, this study has experimentally investigated the thermal behaviour of the erythritol-NaCl PCCs. NaCl has been identified as a potential additive to erythritol as it significantly improved the thermal conductivity of the composites, thereby reducing the charging time. Also, it has been observed that there is an insignificant change in the melting temperature and the activation energy of the PCCs with the addition of NaCl. Further, the DSC-TGA based approach has been inferred to be effective for thermal investigations of PCMs and PCCs as it is systematic providing explicit and implicit estimation of multiple parameters, and hence the methodology is highly recommended for similar investigations. The experimental results were shown as reliable by the comparison with literature reports for erythritol PCMs. Further, the formulated mathematical models and graphical interpretations find applicability in optimizing the

composition and also in the TES system design. From a steam cooking perspective, the synthesized erythritol-PCCs can be envisaged as a potential thermal storage medium that does not degrade at the application temperature.

Acknowledgements: These authors would like to thank the Department of Science and Technology (DST), Government of India and the management of the PSG College of Technology, Coimbatore for their financial support to undertake this project.

REFERENCES

[1] Indora S, Kandpal TC. Institutional cooking with solar energy: A review. *Renew Sustain Energ Rev* 2018;84:131–54. https://doi.org/https://doi.org/10.1016/j.rser.2017.12.001

[2] Motwani K, Patel J. Cost analysis of solar parabolic trough collector for cooking in Indian hostel–a case study. *Int J Ambient Energy* 2019;0(0):1–17. https://doi.org/10.1080/01430750.2019.1653968

[3] Kalogirou SA. Solar thermal collectors and applications. *Prog Energ Combust* 2004;30(3):231-295. https://doi.org/10.1016/j.pecs.2004.02.001

[4] Ravi Kumar K, Krishna Chaitanya NVV, Sendhil Kumar N. Solar thermal energy technologies and its applications for process heating and power generation. *J Clean Prod* 2021;282:125296. https://doi.org/10.1016/j.jclepro.2020.125296

[5] Koçak B, Fernandez AI, Paksoy H. Review on sensible thermal energy storage for industrial solar applications and sustainability aspects. *Sol Energy* 2020;209:135–69. https://doi.org/10.1016/j.solener.2020.08.081

[6] Akba T, Baker D, Yazıcıoğlu AG. Modeling, transient simulations and parametric studies of parabolic trough collectors with thermal energy storage. *Sol Energy* 2020;199:497–509. https://doi.org/10.1016/j.solener.2020.01.079

[7] Ghazouani M, Bouya M, Benaissa M, Anoune K, Ghazi M. Thermal energy management optimization of solar thermal energy system based on small parabolic trough collectors for bitumen maintaining on heat process. *Sol Energy* 2020;211:1403–21. https://doi.org/10.1016/j.solener.2020.10.074

[8] Biencinto M, Bayón R, González L, Christodoulaki R, Rojas E. Integration of a parabolic-trough solar field with solid-solid latent storage in an industrial process with different temperature levels. *Appl Therm Eng* 2021;184:116263. https://doi.org/10.1016/j.applthermaleng.2020.116263

[9] Shchukina EM, Graham M, Zheng Z, Shchukin DG. Nanoencapsulation of phase change materials for advanced thermal energy storage systems. *Chem Soc Rev* 2018;47(11):4156–75. https://doi.org/10.1039/c8cs00099a

[10] Sutjahja IM, Rahman A, Putri RA, *et al.* Electrofreezing of the phase-change material $CaCl_2{\cdot}6H_2O$ and its impact on supercooling and the nucleation time. *Hem Ind* 2019;73(6):363–74. https://doi.org/10.2298/HEMIND190803034S

[11] Jahanpanah M, Sadatinejad SJ, Kasaeian A, Jahangir MH, Sarrafha H. Experimental investigation of the effects of low-temperature phase change material on single-slope solar still. *Desalination* 2021;499:114799. https://doi.org/10.1016/j.desal.2020.114799

[12] Atinafu DG, Ok YS, Kua HW, Kim S. Thermal properties of composite organic phase change materials (PCMs): A critical review on their engineering chemistry. *Appl Therm Eng* 2020;181:115960. https://doi.org/10.1016/j.applthermaleng.2020.115960

[13] Magendran SS, Khan FSA, Mubarak NM, *et al.* Synthesis of organic phase change materials (PCM) for energy storage applications: A review. *Nano-Structures and Nano-Objects* 2019;20:100399. https://doi.org/10.1016/j.nanoso.2019.100399

[14] Singh P, Sharma RK, Ansu AK, Goyal R. Study on thermal properties of organic phase change materials for energy storage. *Mater Today Proc* 2020;28(4):2353–7. https://doi.org/10.1016/j.matpr.2020.04.640

[15] Sharma RK, Ganesan P, Tyagi V V., Metselaar HSC, Sandaran SC. Developments in organic solid-liquid phase change materials and their applications in thermal energy storage. *Energy Convers Manag* 2015;95:193–228. https://doi.org/10.1016/j.enconman.2015.01.084

[16] Atinafu DG, Dong W, Huang X, Gao H, Wang G. Introduction of organic-organic eutectic PCM in mesoporous N-doped carbons for enhanced thermal conductivity and energy storage capacity. *Appl Energy* 2018;211:1203–15. https://doi.org/10.1016/j.apenergy.2017.12.025

[17] Carly F, Vandermies M, Telek S, *et al.* Enhancing erythritol productivity in Yarrowia lipolytica using metabolic engineering. *Metab Eng* 2017;42:19–24. https://doi.org/10.1016/j.ymben.2017.05.002

[18] Coccia G, Aquilanti A, Tomassetti S, Comodi G, Di Nicola G. Design, realization, and tests of a portable solar box cooker coupled with an erythritol-based PCM thermal energy storage. *Sol Energy* 2020;201:530–40. https://doi.org/10.1016/j.solener.2020.03.031

[19] Anish R, Mariappan V, Joybari MM, Abdulateef AM. Performance comparison of the thermal behavior of xylitol and erythritol in a double spiral coil latent heat storage system. *Therm Sci Eng Prog* 2020;15:100441. https://doi.org/10.1016/j.tsep.2019.100441

[20] Yuan M, Ye F, Xu C. Supercooling study of erythritol/EG composite phase change materials. *Energy Procedia* 2019;158:4629–34. https://doi.org/10.1016/j.egypro.2019.01.744

[21] Junior JFR, Oliveski RDC, Rocha LAO, Biserni C. Numerical investigation on phase change materials (PCM): The melting process of erythritol in spheres under different thermal conditions. *Int J Mech Sci* 2018;148:20–30. https://doi.org/10.1016/j.ijmecsci.2018.08.006
[22] Nazzi Ehms JH, De César Oliveski R, Oliveira Rocha LA, Biserni C. Theoretical and numerical analysis on phase change materials (PCM): A case study of the solidification process of erythritol in spheres. *Int J Heat Mass Transf* 2018;119:523–32. https://doi.org/10.1016/j.ijheatmasstransfer.2017.11.124
[23] Rakicka-Pustułka M, Mirończuk AM, Celińska E, Białas W, Rymowicz W. Scale-up of the erythritol production technology – Process simulation and techno-economic analysis. *J Clean Prod* 2020;257:120533. https://doi.org/10.1016/j.jclepro.2020.120533
[24] Fleischer AS. Thermal energy storage using phase change materials: Fundamentals and applications. Springer, Cham, 2015. https://doi.org/10.1007/978-3-319-20922-7
[25] Casini M. Phase-change materials. *Smart Build.* 2016;179–218. https://doi.org/10.1016/B978-0-08-100635-1.00005-8
[26] Kuznik F, Johannes K, David D. Integrating phase change materials (PCMs) in thermal energy storage systems for buildings. Adv. Therm. Energy Storage Syst. Methods Appl. Woodhead Publishing Limited; 2014;325–56. https://doi.org/10.1533/9781782420965.2.325
[27] Yuan M, Ren Y, Xu C, Ye F, Du X. Characterization and stability study of a form-stable erythritol/expanded graphite composite phase change material for thermal energy storage. *Renew Energy* 2019;136:211–22. https://doi.org/10.1016/j.renene.2018.12.107
[28] Shen S, Tan S, Wu S, *et al.* The effects of modified carbon nanotubes on the thermal properties of erythritol as phase change materials. *Energy Convers Manag* 2018;157:41–8. https://doi.org/10.1016/j.enconman.2017.11.072
[29] Wang Y, Wang L, Xie N, Lin X, Chen H. Experimental study on the melting and solidification behavior of erythritol in a vertical shell-and-tube latent heat thermal storage unit. *Int J Heat Mass Transf* 2016;99:770–81. https://doi.org/10.1016/j.ijheatmasstransfer.2016.03.125
[30] Singh R, Sadeghi S, Shabani B. Thermal conductivity enhancement of phase change materials for low-temperature thermal energy storage applications. *Energies* 2019;12(1). https://doi.org/10.3390/en12010075
[31] Sheng N, Dong K, Zhu C, Akiyama T, Nomura T. Thermal conductivity enhancement of erythritol phase change material with percolated aluminum filler. *Mater Chem Phys* 2019;229:87–91. https://doi.org/10.1016/j.matchemphys.2019.02.033
[32] Leng G, Qiao G, Xu G, Vidal T, Ding Y. Erythritol-Vermiculite form-stable phase change materials for thermal energy storage. *Energy Procedia* 2017;142:3363–8. https://doi.org/10.1016/j.egypro.2017.12.471
[33] Oya T, Nomura T, Tsubota M, Okinaka N, Akiyama T. Thermal conductivity enhancement of erythritol as PCM by using graphite and nickel particles. *Appl Therm Eng* 2013;61(2):825–8. https://doi.org/10.1016/j.applthermaleng.2012.05.033
[34] Soni V, Kumar A, Jain VK. Performance evaluation of nano-enhanced phase change materials during discharge stage in waste heat recovery. *Renew Energy* 2018;127:587–601. https://doi.org/10.1016/j.renene.2018.05.009
[35] Qu L. Investigating the Relationship between Salinity and Specific Heat Capacity. *Queensl Acad* n.d. http://nexusstem.co.uk/wp-content/uploads/2017/01/Queensland-Academies-1.pdf
[36] Knowino. Density (chemistry), https://www.tau.ac.il/~tsirel/dump/Static/knowino.org/wiki/Density_(chemistry).html
[37] Brown HM. The thermal conductivity of sodium chloride at elevated temperatures. PhD Thesis, University of Missouri, 1955. https://scholarsmine.mst.edu/cgi/viewcontent.cgi?article=3590&context=masters_theses
[38] Ferguson JB. The melting and freezing point of Sodium Chloride. *J Phys Chem* 1921;26(7):626–30
[39] Zeng JL, Chen YH, Shu L, *et al.* Preparation and thermal properties of exfoliated graphite/erythritol/mannitol eutectic composite as form-stable phase change material for thermal energy storage. *Sol Energy Mater Sol Cells* 2018;178:84–90. https://doi.org/10.1016/j.solmat.2018.01.012
[40] Shin HK, Rhee KY, Park SJ. Effects of exfoliated graphite on the thermal properties of erythritol-based composites used as phase-change materials. *Compos Part B Eng* 2016;96:350–3. https://doi.org/10.1016/j.compositesb.2016.04.033
[41] Vivekananthan M, Amirtham VA. Characterisation and thermophysical properties of graphene nanoparticles dispersed erythritol PCM for medium temperature thermal energy storage applications. *Thermochim Acta* 2019;676:94–103. https://doi.org/10.1016/j.tca.2019.03.037
[42] Shawe J, Riesen R, Widmann J, Schubnell M. Interpreting DSC curves Part 1: Dynamic measurements. 2000. https://www.eng.uc.edu/~beaucag/Classes/Characterization/DSCParts/Artifacts%20in%20DSC%20Usercom_11.pdf
[43] Calculate Activation Energy from TGA data using Origin Software. *Nanoencryption* https://youtu.be/eLqShUApVXM?t=403
[44] Moon B, Jun N, Park S, Seok CS, Hong US. A study on the modified Arrhenius equation using the oxygen permeation block model of crosslink structure. *Polymers (Basel)* 2019;11(1). https://doi.org/10.3390/polym11010136
[45] Peleg M, Normand MD, Corradini MG. The Arrhenius equation revisited. *Crit Rev Food Sci Nutr* 2012;52(9):830–51. https://doi.org/10.1080/10408398.2012.667460
[46] Laidler KJ. The development of the arrhenius equation. *J Chem Educ* 1984;61(6):494–8. https://doi.org/10.1021/ed061p494
[47] Camirand CP. Measurement of thermal conductivity by differential scanning calorimetry. *Thermochim Acta* 2004;417(1):1–4. https://doi.org/10.1016/j.tca.2003.12.023

[48] Camirand C. Étude de la chaleur spécifique et de la conductivité thermique des hydrures métalliques par calorimétrie différentielle. Thèse et mémoire, Université du Québec à Trois-Rivières, 2000. https://depot-e.uqtr.ca/id/eprint/3139 in French
[49] Flynn JH, Levin DM. A method for the determination of thermal conductivity of sheet materials by differential scanning calorimetry (DSC). *Thermochim Acta* 1988;126:93–100. https://doi.org/10.1016/0040-6031(88)87254-X
[50] Niezgoda-Zelasko B. The Enthalpy-porosity Method Applied to the Modelling of the Ice Slurry Melting Process during Tube Flow. *Procedia Eng* 2016;157:114–21. https://doi.org/10.1016/j.proeng.2016.08.346
[51] Eanest Jebasingh B, Valan Arasu A. A comprehensive review on latent heat and thermal conductivity of nanoparticle dispersed phase change material for low-temperature applications. *Energy Storage Mater* 2020;24:52–74. https://doi.org/10.1016/j.ensm.2019.07.031
[52] Okoro HK, Odebunmi EO. Kinetics and mechanism of oxidation of sugar and sugar alcohols by KMnO4. *Int J Phys Sci* 2009;4(9): 673ED0819348. https://doi.org/10.5897/IJPS.9000340
[53] Mayilvelnathan V, Valan Arasu A. Experimental investigation on thermal behavior of graphene dispersed erythritol PCM in a shell and helical tube latent energy storage system. *Int J Therm Sci* 2020;155:106446. https://doi.org/10.1016/j.ijthermalsci.2020.106446
[54] Gunasekara SN, Stalin J, Marçal M, *et al.* Erythritol, glycerol, their blends, and olive oil, as sustainable phase change materials. *Energy Procedia* 2017;135:249–62. https://doi.org/10.1016/j.egypro.2017.09.517
[55] MINITAB. Interpolation method for mesh. *MINITAB*. https://support.minitab.com/en-us/minitab/18/help-and-how-to/graphs/how-to/general-graph-options/display-options/interpolation-method-for-mesh/

Diferencijalna skenirajuća kalorimetrijska ispitivanja faznopromenljivog kompozita eritritol – natrijum hlorid za primenu u skladištenju toplotne energije

Paul Gregory Felix, Velavan Rajagopal i Kannan Kumaresan

Univerzitet PSG College of Technology, Coimbatore, India

(Naučni rad)

Izvod

Zbog niske toplotne provodljivosti organskih faznopromenljivih materijala (phase change materials-PCM), njihova primena u sistemima za skladištenje toplotne energije zahteva korišćenje odgovarajućih tehnika radi poboljšanje prenosa toplote. Cilj ove studije je bio poboljšanje toplotne provodljivosti eritritola kao faznopromenljivog materijala, korišćenjem natrijum-hlorida (NaCl) kao aditiva, tako da se materijal može primeniti za sisteme za kuvanje na pari kada je integrisan sa solarnim paraboličnim kolektorima. Eritritol-NaCl smeše su sintetisane metodom topljenja, a ključne fizičko-hemijske osobine smeše su određene primenom diferencijalne skenirajuće kalorimetrije (DSC) u kombinaciji sa termo-gravimetrijskom analizom (TGA). Resultati pokazuju da je došlo do značajnog poboljšanja toplotne provodljivosti eritritola sa dodatkom NaCl u odnosu na čist eritritol. Takođe, termičko ponašanje materijala ukazuje na to da je pogodan za kuvanje na pari. Razvijeni matematički modeli zasnovani na eksperimentalnim rezultatima u ovoj studiji, mogu se potencijalno koristiti za dalja istraživanja kompozita eritritol-NaCl.

Ključne reči: kompoziti (smeša); skladištenje latentne toplote; matematičko modelovanje; kuvanje na pari; toplotna provodljivost